ARTICLE

DFT Study on Structural Distortion and Vibronic Coupling of Vanadyl Porphyrin Anion and Cation

Hui-ling Gao, Fang Chen, Guo-hua Yao, Dong-ming Chen*

Department of Chemical Physics, University of Science and Technology of China, Hefei 230026, China

(Dated: Received on May 11, 2013; Accepted on May 20, 2013)

The geometries of one-electron reduced/oxidized species ($[TOP]^-/[VOP]^+$) of vanadyl porphyrin (VOP) have been calculated with PBE1PBE method. The results show that for both $[VOP]^-$ and $[VOP]^+$ the ground states are triplet, in which one of the two unpaired electron occupies the d_{xy} orbital of the V atom while the other occupies the π-orbital of porphyrin ring. Thus both $[VOP]^-$ and $[VOP]^+$ can be considered as π-radicals. The ground state of neutral VOP molecule is doublet with the unpaired electron occupying d_{xy} orbital of V atom. In contract to the C_{4v} symmetry of neutral VOP molecule, $[VOP]^-$ anion has a "rectangular" distorted C_{2v} structure due to Jahn-Teller effect. The linear vibronic coupling constants for the Jahn-Teller active modes of $[TOP]^-$ were evaluated and the node patterns of frontier KS orbitals are used to explain the reason why the distortion occurs along specific modes. The ground state $[VOP]^+$ has a porphyrin ring with pronounced bond length alternation due to pseudo-Jahn-Teller effect, causing its symmetry declined from C_{4v} to C_4. The bond length alternation is well explained with the node patterns of re-constructed frontier KS orbitals.

Key words: Vanadyl porphyrin, Jahn-Teller effect, Vibronic coupling

I. INTRODUCTION

Metalloporphyrin (MP) radicals play a crucial role in many important biological processes [1−4]. The chemical basis for the biological functions of metalloporphyrins originates from their versatility in redox and coordination properties. In recent years, the porphyrins and their analogues also receive increasing interests as new molecular conducting/semiconducting materials and photo-functional materials. As molecular conductors/semiconductors, doping with cations or anions into porphyrin-based materials is an effective route to modulate their electric properties. As sensitizing dye, the excited state charge-transfer of the porphyrins is closely connected to the opt-electric conversion efficiency of devices. It is clear that investigation on the redox properties of porphyrins and the structures of porphyrin radicals is crucial not only for understanding the mechanisms of biological charge-transfer processes of porphyrin prosthetic groups but also for developing metalloporphyrin-based new materials. For these reasons, the metalloporphyrin radicals have been extensively studied using various spectroscopic methods [5−8], X-ray crystallography [9, 10], and theoretical calculations [11−16].

Vanadyl porphyrin (VOP) derivatives extensively exist in the crude oil and oil-shale. In industry, the contents and distributions of VOPs are used to evaluate the organic matter maturity and the quality of source-rocks [17−19]. VOPs are also used as organic optical sensors [20−22]. In addition, owing to the stable coordination of axial oxygen atom, VOPs are also important structural models to mimic the active centers of peroxidase and other heme proteins [2, 3, 23, 24]. The redox states and electron-transfer of VOPs with peripheral substituents have been studied by using UV-Vis and resonance Raman spectroscopy [23, 24]. Theoretical calculations of neutral VOPs and related compounds using DFT have been reported recently, with the concerns mainly on the ground state structures and their bonding/interaction with axially coordinated small molecules [25−28]. The redox species of VOPs, on the other hand, have been seldom studied by theoretical calculation.

In the present work, geometric and electronic structures of one-electron reduced/oxidized VOPs ($[VOP]^-$ and $[VOP]^+$) are calculated with DFT method to reveal the structural distortion and vibronic coupling in these systems and to provide a deeper understanding of related spectroscopic phenomena.

II. COMPUTATIONAL METHODS

DFT calculations for the structural optimizations of VOP, $[VOP]^-$, and $[VOP]^+$ were carried out by using the Perdew-Burke-Ernzerhof's one-parameter hy-

*Author to whom correspondence should be addressed. E-mail: dmchen@ustc.edu.cn, Tel.: +86-551-63606145

TABLE I Relative total energies (in kJ/mol) of VOP, $[VOP]^-$, and $[VOP]^+$ calculated with PBE1PBE[a].

Species	Symmetry	State	Core shape[b]	$\langle S^2\rangle$[c]	ΔE/(kJ/mol)	Imaginary frequency/cm^{-1}
$[VOP]^-$	C_{2v}	$^3B_1$	Rectangular	2.0287	0.0	No
$[VOP]^-$	C_{2v}	$^3B_2$	Rhombic	2.0554	1.8	i668
$[VOP]^-$	C_s	$^1A'$	Trapezoid	0	108.6	No
VOP	C_{4v}	$^2B_1$	Square	0.7666	113.1	No
VOP	C_{2v}	$^4B_1$	Rectangular	3.7864	287.9	No
$[VOP]^+$	C_4	^3B	Square	2.0496	765.2	No
$[VOP]^+$	C_{4v}	$^3B_2$	Square	2.0693	765.4	i315
$[VOP]^+$	C_{4v}	$^3B_1$	Square	2.0759	769.2	i778
$[VOP]^+$	C_{2v}	$^1A_1$	Rhombic	0	811.5	No

[a] Basis sets: 6-31G(d) for C, N, O, and H; TZVP for V.
[b] Shape of porphyrin core was defined by four meso-carbon (C_m) atoms.
[c] Expectation value of the square of total electronic spin.

brid functional (referred as PBE1PBE, also known as PBE0) [29]. Standard 6-31G(d) basis sets were used for C, N, O, and H, while Ahlrichs' TZVP basis sets were for V atom [30]. Analytic frequency calculations at the optimized geometries were conducted at the same level of theory as optimization to confirm the structure to be an energy minimum (with all the frequencies to be positive) or an transition structure (with a single imaginary frequency). Assignment of individual vibrational frequency has been carried out by inspecting the calculated Cartesian displacements of the corresponding normal mode. All calculations were performed with the Gaussion 09 [31] program suite on the Lenova 1800 supercomputer of USTC supercomputation center.

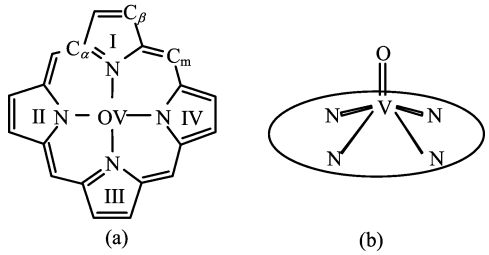

FIG. 1 (a) Structural sketch of VOP with the symbols of the atoms. (b) Side-view sketch of VOP showing the orientation of the vanadium and oxygen atoms.

III. RESULTS AND DISCUSSION

A. Ground state geometry and electronic structure of neutral VOP molecule

Geometric optimizations and frequency calculations are carried out for the doublet and quartet states of neutral VOP molecule, singlet and triplet states of $[VOP]^+$ cation and $[VOP]^-$ anion. Table I lists the relative energies and expectation values of total electron spin for the studied species. From Table I, it can be found that the spin contamination is not severe and should not cause significant problem to the calculation results. For the convenience of expression, the shapes of porphyrin ring in Table I (rectangular, rhombic, square, and trapezoid) are defined with the positions of four C_m atoms. For a "rectangular" structure there are two σ_V planes passing through V, O, and the N atoms of the opposite pyrrole rings, while for a "trapezoid" one there exists only one such plane. For a "rhombic" structure, the two σ_V planes pass V and O atoms as well as each pair of the opposite C_m atoms.

Figure 1 displays the molecular sketch of VOP. Due to the axial ligation of the oxygen atom, the porphyrin macrocycle shows slight doming deformation. The neutral VOP contains 191 electrons and thus is an open-shelled system which may be doublet or quartet. Table II lists selected structural parameters of VOP, $[VOP]^-$, and $[VOP]^+$ in most stable electron multiplicities. PBE1PBE optimized doublet VOP has C_{4v} symmetry with four equal N−V bonds (2.0845 Å). The derivation of the V atom from plane of four nitrogen atoms (denoted as the N4 plane) is 0.5216 Å. The V−O bond distance is 1.5665 Å, which consists well with the experimental data [32]. The quartet state has C_{2v} symmetry (rectangular) with the four N−V bonds to be 2.0962, 2.0935, 2.0962, and 2.0935 Å, respectively. For the quartet state VOP, the V−O bond distance is 1.5632 Å and the distance between the V atom and the center of four N atoms is 0.4991 Å. The total energy of the quartet state is significantly higher than the doublet by 174.8 kJ/mol, indicating the doublet to be the ground state of VOP.

Figure 2 shows the contour diagrams for the frontier Kohn-Sham orbitals of doublet VOP molecule. It can be seen from Fig.2 that the singly occupied orbital (SOMO, $9b_1$) is mainly composed of the d_{xy} orbital of V(IV) ion and is basically a non-bonding orbital in character. SOMO-1 and SOMO-2 are nearly degenerate $21a_1$ and $6a_2$, respectively. For normal four-coordinated

DOI:10.1063/1674-0068/26/05/504-511

TABLE II Selected structural parameters of the most stable structures of $[VOP]^-$, $[VOP]^+$, and VOP by PBE1PBE calculation. Bond distances in Å, bond angles in (°).

	$[VOP]^-(C_{2v})^{a,b}$	$[VOP]^+(C_4)^{a,c}$	$VOP(C_{4v})^d$
$C_\beta-C_\beta$	1.3555, 1.3810	1.3512	1.3599
$C_\beta-C_\alpha$	1.4448, 1.4174	1.4518, 1.4495	1.4368
$C_\alpha-N$	1.3776, 1.3742	1.3785, 1.3560	1.3696
$C_\alpha-C_m$	1.3751, 1.4079	1.3751, 1.4045	1.3881
V−N	2.0826, 2.1010	2.0800	2.0845
V−O	1.5740	1.5601	1.5665
$d_{V-Ct}{}^e$	0.5175	0.5190	0.5216
$C_\beta-C_\beta-C_\alpha$	107.1, 106.7	106.6, 106.7	106.8
$C_\beta-C_\alpha-N$	109.7, 110.3	109.9, 110.8	110.2
$C_\alpha-N-C_\alpha$	106.4, 106.0	105.9	106.1
$C_\alpha-C_m-C'_\alpha$	125.7	125.2	125.6
N−V−N	86.5	86.4	86.4
N−V−O	104.4	104.4	104.5

[a] Triplet state.
[b] Rectangular distorted Jahn-Teller ground state.
[c] Pseudo-Jahn-Teller ground state.
[d] Doublet state.
[e] Distance between the V atom and the center of N4 core.

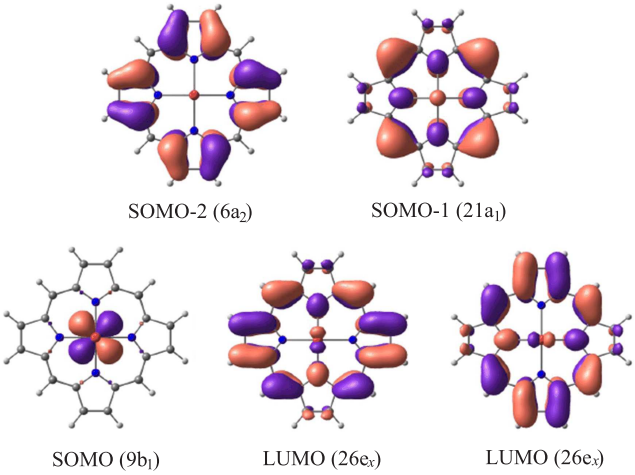

FIG. 2 The contour diagrams of the frontier Kohn-Sham orbitals of VOP.

planar metalloporphryins, these two orbitals belong to a_{2u} and a_{1u} symmetries, respectively, according to the irreducible representations of D_{4h} point group. It is noticed that $21a_1$ and $6a_2$ are constructed by the p_z orbitals of the C and/or N atoms and thus can be attributed to the delocalized π orbitals of the porphyrin macrocycle. The LUMO is doubly degenerate 26e (e_g symmetry according to the D_{4h} point group), which also belongs to the π system of the porphyrin ring.

It is noteworthy that the compositions of SOMO-1, SOMO-2, and LUMO of VOP are quite similar to the HOMO, HOMO-1, and LUMO of ZnP (a typical four-coordinate planar metalloporphyrin). Therefore, it is not surprising that the VOPs have similar electronic absorption spectra as normal four-coordinate metalloporphyrins [33, 34].

In the following sections, we will see that the one-electron oxidation/reduction of VOP involves mainly the π-system of the porphyrin macrocycle (*i.e.*, the $21a_1/6a_2$ and 26e orbitals) while the $9b_1$ (*i.e.*, the d_{xy} of V(IV) ion) orbital maintains singly occupied. Thus the one-electron reduced (or oxidized) product of VOP can be considered as a π-radical anion (or a π-radical cation).

B. Jahn-Teller distortion of $[VOP]^-$ anion

Spiro *et al.* have studied the UV-Vis absorption and resonance Raman spectra of electrochemically reduced vanadyl octaethylporphyrin ($[VOOEP]^-$) [33]. It was suggested that the electrochemically reduced species was π-radical. The resonance Raman spectrum of $[VOOEP]^-$ showed significant variations in comparison with the neutral molecule. For instance, the depolarization ratios of the totally symmetric modes (A_{1g}) were increased while those of non-totally symmetric modes (B_{1g}) decreased. The Raman intensities of B_{1g} modes were increased considerably, hinting a Frank-Condon type enhancement. The A_{1g} and B_{1g} modes which have the same local coordinates show unusual differences in vibrational frequencies. For the instance of $C_\beta-C_\beta$ stretching vibrations, the frequency difference between the A_{1g} and B_{1g} modes was found to be unusually increased by as large as 40 cm^{-1}. From these experimental phenomena, it was concluded that compared with the neutral VOOEP, the symmetry of $[VOOEP]^-$ anion decreased and the fourth-ford axis lost. This symmetry breaking of $[VOOEP]^-$ was attributed to the Jahn-Teller (JT) effect that caused structural deformation mainly along the B_{1g} normal coordinates [33]. Besides $[VOOEP]^-$, the JT distortion along the B_{1g} modes was also found for vanadyl tetraphenylporphyrin anion ($[VOTPP]^-$) from the Raman experiments [34].

Geometry optimization have been conducted for the singlet and triplet states of $[VOP]^-$ anion. The results manifest that the singlet state belongs to the C_s point group with the reflection mirror passing through the oxygen and vanadium atoms and a pair of N atoms on the opposite pyrrole rings. The V−O bond-length is 1.5792 Å and the distance between the V atom and the center of four N atoms is 0.5283 Å. The four N−V bond distances are 2.0772, 2.0772, 2.0777, and 2.1426 Å respectively, hinting that the V(IV) ion bonds tightly with three of the four N atoms while loosely with the rest one.

Under C_{4v} symmetry, triplet $[VOP]^-$ has the electronic configuration $(9b_1)^1(26e)^1$, with the two unpaired electrons occupying $9b_1$ (the d_{xy} non-bonding orbital of V^{4+}) and 26e (π-orbital of the porphyrin ring),

DOI:10.1063/1674-0068/26/05/504-511

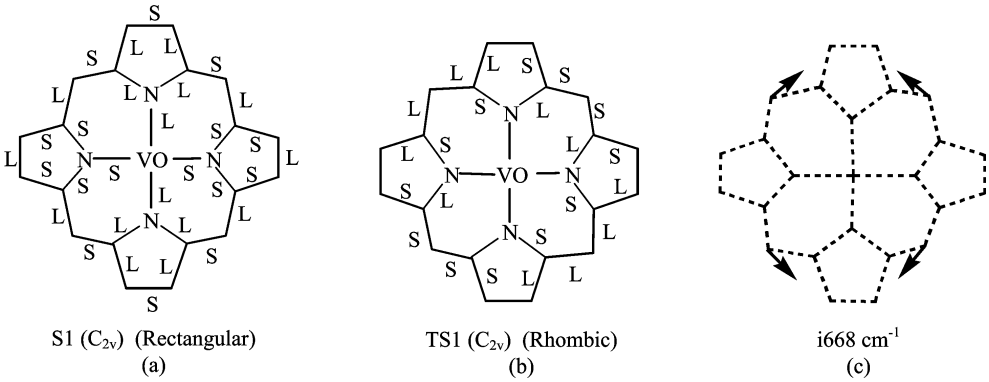

FIG. 3 Schematic diagrams of triplet $[VOP]^-$ anion showing (a) the steady structure (S1, rectangular), (b) the transition state (TS1, rhombic), in which the letters L and S indicate the corresponding bonds are increased and decreased in comparison with the average values, and (c) the nuclear motions along the reaction coordinate of the transition state (TS1).

respectively. Thus the term symbol of the electronic state is ^{3}E. As doubly degenerate 26e is occupied with one electron, Jahn-Teller distortion is expected to occur so as to relieve the degeneration. Geometric optimization of triplet $[VOP]^-$ obtains two stationary structures, both belong to C_{2v} point group. The two stationary structures of triplet $[VOP]^-$ are denoted as S1 (rectangular) and TS1 (rhombic), respectively. Figure 3 (a) and (b) shows the sketches for the rectangular and rhombic structures of triplet $[VOP]^-$, in which the letters L or S indicate that the corresponding bonds are increased or decreased in comparison with the average values.

It can be seen from Table I that the energy of singlet $[VOP]^-$ higher than the rectangular and rhombic triplet by 108.6 and 106.8 kJ/mol, respectively, indicating the rectangular triplet to be the ground state of $[VOP]^-$. Due to the symmetry breaking caused by J-T effect, the rectangular triplet displays significant alteration on bond-lengths. The $C_\beta-C_\beta$ bonds of pyrrole rings I and III are shorter than those of the pyrrole rings II and IV by 0.0255 Å, while the $C_\alpha-C_\beta$ bonds of rings I and III are longer than those of the pyrrole rings II and IV by 0.0274 Å. The difference in bond-length between two adjacent $C_\alpha-C_m$ bonds is 0.0328 Å. The difference between the $C_\alpha-N$ bonds is only 0.0034 Å, indicating a small influence of JTE on the $C_\alpha-N$ bonds. Analytical frequency calculations reveal that the rectangular triplet (S1) has no imaginary frequency and thus is an energy minimum of the potential energy surface (PES). On the other hand, the rhombic triplet (TS1) produces single imaginary frequency (i668 cm^{-1}). Moreover, the atomic displacements of this imaginary frequency indicate that it is the transition state connecting two conjugate structures of rectangular triplet. In view of the very small barrier (only 1.8 kJ/mol) of TS1, it is believed that in the triplet state $[VOP]^-$ can easily interconverse between two conjugate rectangular structures.

Analysis of the vibronic coupling in a J-T system provides information about how the electronic state controls the nuclear displacements from the original high symmetry structure to the lower one. For the case of $[VOP]^-$, the linear vibronic coupling constant between the ^{3}E electronic state and the mth J-T active B_1 mode $g_{B_1,m}$ can be expressed as [15, 16, 36]:

$$g_{B_1,m} = \frac{\pi}{h\omega_m}\left\langle E\left|\frac{\partial\hat{V}}{\partial q_{B_1,m}}\right|E\right\rangle \tag{1}$$

here, $q_{B_1,m}$ is the dimensionless normal coordinate of the mth B_1 normal mode of the frequency ω_m, which is related to the normal coordinate $Q_{B_1,m}$ by:

$$q_{B_1,m} = \sqrt{\frac{2\pi\omega_m}{h}}Q_{B_1,m} \tag{2}$$

where ω_m is the modes' frequency in reciprocal centimeters.

In order to evaluate the vibronic constants, a fictitious high symmetry structure needs to be used as the reference. In the present work we use a C_{4v} structure, which is averaged from two conjugated rectangular structures of $[VOP]^-$ triplet, as the reference structure. The energy difference between this C_{4v} reference structure and the JT-stabilized rectangular structure is 7.44 kJ/mol. This value is significantly larger than the room temperature thermal energy (about 2.48 kJ/mol), indicating that the JTE of triplet $[VOP]^-$ can be considered as a static effect in a Raman process as pointed out by Spiro *et al.* [33, 34]. The normal coordinates of VOP neutral molecule is used to describe the directions of structural distortion. The derivatives of the total energy (calculated using tight SCF convergence criteria) with respective to the normal modes can be computed by slightly distorting the C_{4v} reference structures along each B_1 normal coordinate. The vibronic coupling constants can be evaluated from the gradient of the total energy curve near the undistorted C_{4v} reference structure [15, 16].

Figure 4 shows the change of total energy of $[VOP]^-$ anion via the distortion along selected J-T active nor-

DOI:10.1063/1674-0068/26/05/504-511

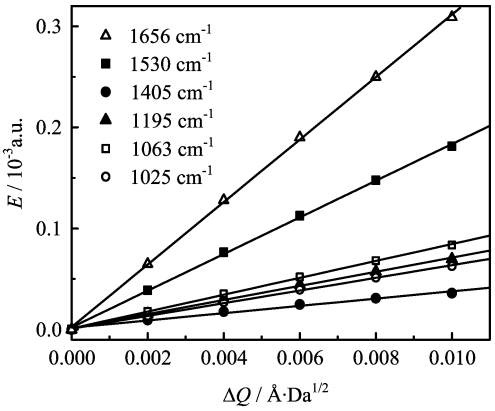

FIG. 4 Change of total energy of $[VOP]^-$ via the distortions along selected J-T active normal modes. Energies E were calculated with PBE1PBE/6-31G(d)-TZVP.

mal coordinates. The calculated linear vibronic coupling constants of the J-T active modes (B_1 modes) are listed in Table III. In Table III the calculated frequencies have been scaled by 0.97, a factor suitable for metalloporphyrins and related compounds [37, 38]. The symbol and the local-coordinate description for each vibrational mode in Table III follow those used in the vibrational analysis of other metalloporphyrins [39, 40].

The highest-frequency 3192 cm^{-1} mode in Table III is due to the $C_\beta-H_\beta$ stretch vibration (ν_{14}). The 1405 and 1063 cm^{-1} modes are due to the in-plane bending vibrations of bending vibrations of C_m-H_m (ν_{13}) and $C_\beta-H_\beta$ (ν_{17}), respectively. The 1656, 1530, 1195, and 733 cm^{-1} modes are assigned to the asymmetric stretch of $C_\alpha-C_m$ bonds (ν_{10}), $C_\beta-C_\beta$ stretch (ν_{11}), symmetric pyrrole half-ring stretch (ν_{12}), and pyrrole in-plane deformation (ν_{16}), respectively. The low frequency vibration at 200 cm^{-1} is assigned to the in-plane pyrrole-translational mode (ν_{18}). The frequencies at 785, 661, 269, and 54 cm^{-1} are due to the out-of-plane modes assigned to $C_\beta-H_\beta$ wag, symmetric pyrrole folding, pyrrole tilting, and pyrrole out-of-plane translation.

As shown in Table III, the ν_{10}, ν_{11}, and ν_{18} modes have large coupling constants while the ν_{14}, ν_{13}, and γ_{17} have quite small coupling constants. The large coupling constants of ν_{11} mode can be explained from the nodal pattern of the singly occupied 26e orbital. Given that a single electron occupies one component of 21e, the valence configuration of $[VOP]^-$ is either $(9b_1)^1(26e_x)^1(26e_y)^0$ or $(9b_1)^1(26e_x)^0(26e_y)^1$. As shown in Fig.2, for the $26e_x$ orbital, the $C_\beta-C_\beta$ bonds of pyrrole rings I and III are weakly bonding in character while those of the pyrrole rings II and IV are strongly anti-bonding. Similarly, one of the two adjacent $C_\alpha-C_m$ bonds is bonding in character while the other is anti-bonding. Thus the motion of the nuclei along the ν_{11} and ν_{10} modes can effectively modulate the relative energy level of $26e_x$ and $26e_y$. On the other hand, ν_{14}, ν_{13}, and γ_{17} have small coupling constants since the H_β and H_m atoms do not observably contribute to the $26e_x/26e_y$ orbital. Unlike ν_{14}, ν_{13}, and γ_{17}, the ν_{17} mode (1063 cm^{-1}) has a rather large coupling constant (0.168) although it is assigned to the $C_\beta H_\beta$ in-plane bending. However, from its atomic Cartesian displacements we find that in the ν_{17} mode the $C_\beta H_\beta$ in-plane bending is strongly coupled to the $C_\beta-C_\beta$ stretch. Thus the rather large coupling constant of ν_{17} seems borrowed from ν_{11}. The 661 cm^{-1} mode (symmetric pyrrole folding) has a very small coupling constant (0.01). This seems reasonable as the folding of the pyrrole rings is expected to destroy the porphyrin π-system. It is interesting that out-of-plane modes γ_{16} (269 cm^{-1}) and γ_{18} (54 cm^{-1}) have quite large coupling constants. From atomic motions of these two modes, it is revealed that, while they are nominally assigned to out-of-plane modes, they do involve pyrrole translational motion in a similar way to the in-plane ν_{18} mode. Clearly the very large coupling constant of the γ_{18} mode should also be attributed to its small frequency (54 cm^{-1}), according to Eq.(1) and Eq.(2), which leads to a large coupling constant even for a small energy change.

TABLE III Calculated vibronic coupling constants ($g_{B_1,m}$) for the J-T active B_1 modes of $[VOP]^-$.

No.[a]	ω_m/cm^{-1}	$g_{B_1,m}$	Assign[b]
1	54	0.740	γ_{18} γ(Pyr transl)
8	200	0.271	ν_{18} ν(Pyr transl)
13	269	0.163	γ_{16} γ(Pyr tilt)
28	661	0.010	γ_{15} γ(Pyr fold)$_s$
37	733	0.196	ν_{16} δ(Pyr def)
43	785	0.023	γ_{17} $\gamma(C_\beta-H_\beta)$
60	1025	0.136	ν_{15} ν(Pyr br)
66	1063	0.168	ν_{17} $\delta(C_\beta H_\beta)$
72	1195	0.123	ν_{12} ν(Pyr/2)
84	1405	0.060	ν_{13} $\delta(C_mH_m)$
89	1530	0.211	ν_{11} $\nu(C_\beta C_\beta)$
96	1656	0.311	ν_{10} $\nu(C_\alpha C_m)_{as}$
105	3192	0.002	ν_{14} $\nu(C_\beta H_\beta)$

[a] Mode number within total 108 normal modes (in the sequence of the increase of frequency).
[b] Mode descriptions according to Refs.[39, 40].

C. The pseudo-Jahn-Teller distortion of $[VOP]^+$

PBE1PBE calculation indicated that the energy of singlet $[VOP]^+$ is higher than that of the triplet by 42−46 kJ/mol (Table I), indicating that the ground state of $[VOP]^+$ is triplet. The singlet $[VOP]^+$ belongs to the C_{2v} point group with the two reflection planes passing the O and V atoms as well as each pair of opposite C_m atoms. The four N atoms in singlet

DOI:10.1063/1674-0068/26/05/504-511

$[VOP]^+$ are coplanar while the four C_m atoms locate alternatively up and down the N_4 plane, resulting significant out-of-plane saddling distortion. The N−V and V−O bond lengths in singlet $[VOP]^+$ are 2.0146 and 1.5474 Å, respectively. For the triplet state $[VOP]^+$, geometric optimizations with the constraint of C_{4v} group generate two stationary structures by using slightly different starting geometries. They are $^3B_2$ and $^3B_1$ electronic states, respectively, with the former to be slightly more stable than the later (by 3.8 kJ/mol). However, frequency calculations at the optimized structures show that both C_{4v}-$^3B_2$ and C_{4v}-$^3B_1$ are not stable and both have an imaginary frequency (i315 cm^{-1} for C_{4v}-$^3B_2$ and i778 cm^{-1} for C_{4v}-$^3B_1$). The atomic Cartesian displacements of the two imaginary frequencies are quite similar and both of them can be considered as the porphyrin in-plane pseudo-rotational vibrations (A_2 symmetry under C_{4v} point group or A_{2g} symmetry under D_{4h} point group).

From either C_{4v}-$^3B_2$ or C_{4v}-$^3B_1$ structures, re-optimization along the coordinate of imagination frequency produces the same structure with C_4 symmetry. The total energy of new structure is lower than those of C_{4v}-$^3B_2$ and C_{4v}-$^3B_1$ by 0.2 and 4.0 kJ/mol, respectively. Frequency calculation of the new structure gives rise to positive values for all normal modes, indicating the obtained structure to be the true ground state of $[VOP]^+$ cation. The symmetry lowering of $[VOP]^+$ from C_{4v} to C_4 is thought to be attributable to the pseudo-Jahn-Teller (pJT) distortion which is expected to occur when two electronic states are nearly degenerate, as the case of C_{4v}-$^3B_2$ and C_{4v}-$^3B_1$ states of $[VOP]^+$. The pJT effect of porphyrin π-radical cations has been originally measured from the resonance Raman experiments [24] and later on been used to explain the crystallographic data of porphyrin π-radical cations [10].

The structural parameters of pJT distorted triplet $[VOP]^+$ (C_4 point group) are listed in Table II. The N−V and V−O bond distances are 2.0800 and 1.5601 Å, respectively. The four N atoms are coplanar while the V atom locates up the N4 plane by 0.5190 Å. Figure 5 (a) and (b) illustrates the structure charge of triplet $[VOP]^+$ (C_4 structure) and the atomic Cartesian displacements for the i315 cm^{-1} mode of C_{4v}-$^3B_2$ structure. The porphryin ring of the triplet displays significant alteration for the bond-lengths due to the symmetry lowering. For instance, in the same pyrrole five-membered ring, one C_α−N bond-length is larger than another by 0.0225 Å. The difference in bong-lengths between two adjacent C_α−C_m bonds is 0.0294 Å. The pJT effect has only weak influence on the C_α−C_β bonds as manifested by the quite small difference (0.0023 Å) in bong-lengths for each pair of C_α−C_β bonds in the same pyrrole ring.

With the frame of C_{4v} symmetry, the pJT effect of triplet $[VOP]^+$ is considered to be originated from the interaction between the $(9b_1)^1(21a_1)^1$ and $(9b_1)^1(6a_2)^1$

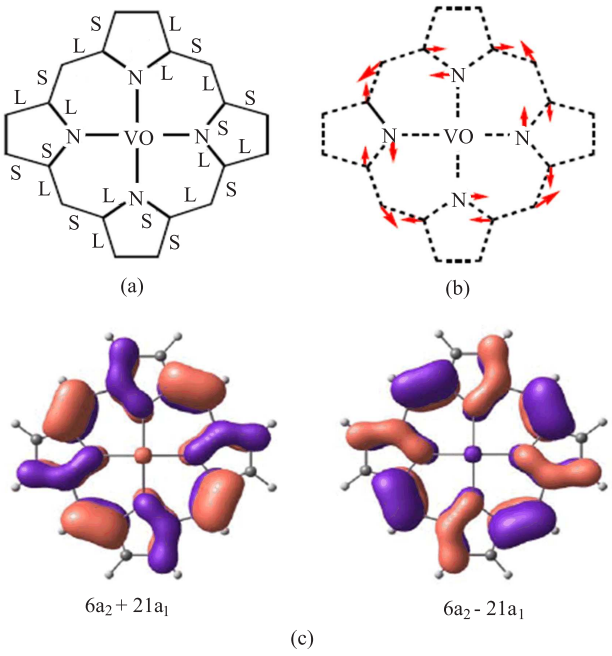

FIG. 5 Schematic illustration for the pJT effect of triplet $[VOP]^+$. (a) The structure of symmetry-broken pJT ground state (C_4 group), where the letters L and S indicate the corresponding bonds are increased or decreased in comparison with the average values. (b) The nuclear motions corresponding to the i315 cm^{-1} imaginary frequency of the $^3B_2$ state of $[VOP]^+$ (C_{4v} group). (c) In-phase and opposite-phase 50:50 combinations of $6a_2$ and $21a_1$ orbitals.

configurations which are mixed by the vibronic perturbation. Assuming a 50:50 mixing of the two configurations and frozen of other orbitals, both the $21a_1$ and $6a_2$ orbitals can be considered as half populated. Thus the in-phase and/or opposite-phase combinations of the $21a_1$ and $6a_2$ orbitals provide an intuitional description of the overall bonding characteristic of the π-system. As shown in Fig.5(c), the in-phase or opposite-phase combinations of the $21a_1$ and $6a_2$ orbitals cause one of the adjacent C_α−C_m bonds to be bonding in character while the other to be anti-bonding. Similarly, one of the two C_α−N bonds in the same pyrrole ring is bonding while the other is anti-bonding. Especially, the pairs of C_α−C_m bonds and C_α−N bonds, which show large alteration in the bond-lengths, are consistent with the change from bonding to anti-bonding. On the other hand, the small bond-length alteration of the pair of C_α−C_β bonds consists with bonding to non-bonding change. Moreover, the nodal pattern of Fig.5(c) corresponds well to the short-long alteration in the bond-lengths in Fig.5(a).

We have tried to calculate the vibronic coupling constants of $[VOP]^+$ triplet with the C_{4v}-$^3B_1$/C_{4v}-$^3B_2$ averaged structure as the reference structure. However, we found that the total energy was very insensitive to the variation of geometry nearby the reference configuration, which seems to result from the small pJT stabi-

DOI:10.1063/1674-0068/26/05/504-511

lization energy. It seems that, in order to obtain convincible vibronic coupling constants of $[VOP]^+$ triplet, new computational methods with the precision much higher than the present one should be used.

IV. CONCLUSION

We have theoretically studied the ground state structures of neutral molecule and one-electron reduced/oxidized products of VOP at the PBE1PBE level of theory. It is found that both $[VOP]^-$ and $[VOP]^+$ have triplet ground states which can be considered as π-radical anion/cation. Due to the Jahn-Teller effect, $[VOP]^-$ has a rectangular-distorted structure belonging to C_{2v} point group. The two conjugated Jahn-Teller structures inter-converse to each other with a rhombic transition structure. The linear coupling constants of the Jahn-Teller active modes are calculated. The triplet $[VOP]^+$ also shows distortion from C_{4v} symmetry to C_4 due to the pseudo-Jahn-Teller effect caused by the near degeneration of electronic structures. The structural distortions of both $[VOP]^-$ and $[VOP]^+$ can be rationalized with the nodal patterns of frontier Kohn-Sham orbitals.

V. ACKNOWLEDGMENTS

This work was supported by the National Education Department of China (No.200803580022) and the Supercomputation Center of University of Science and Technology of China.

[1] M. Sono, M. P. Roach, E. D. Coulter, and J. H. Dawson, Chem. Rev. **96**, 2841 (1996).
[2] J. T. Groves, K. Shalyaev, and J. Lee, *The Porphyrin Handbook*, Vol. 4, 1st Edn, K. M. Kadish, K. M. Smith, and R. Guilard, Eds., San Diego: Academic Press, 17 (2000).
[3] Y. Watanabe, *The Porphyrin Handbook*, Vol. 4, 1st Edn, K. M. Kadish, K. M. Smith, and R. Guilard, Eds., San Diego: Academic Press, 97 (2000).
[4] J. Fajer and M. S. Davis, *The Porphyrins*, Vol. 3, 1st Edn, D. Dolphin Ed., New York: Academic Press, 197 (1978).
[5] I. Morishima, Y. Takamuki, and Y. Shiro, J. Am. Chem. Soc. **106**, 7666 (1984).
[6] G. M. Godziela and H. M. Goff, J. Am. Chem. Soc. **108**, 2237 (1986).
[7] R. S. Czernuszewicz, K. A. Macor, X. Y. Li, J. R. Kincaid, and T. G. Spiro, J. Am. Chem. Soc. **111**, 3860 (1989).
[8] W. A. Oertling, A. Salehi, C. K. Chang, and G. T. Babcock, J. Phys. Chem. **93**, 1311 (1989).
[9] H. S. Song, R. D. Orosz, C. A. Reed, and W. R. Scheidt, Inorg. Chem. **29**, 4274 (1990).
[10] W. R. Scheidt, J. Bio. Inorg. Chem. **6**, 727 (2001).
[11] K. Prendergast and T. G. Spiro, J. Phys. Chem. **95**, 9728 (1991).
[12] A. G. Skillman, J. R. Collins, and G. H. Loew, J. Am. Chem. Soc. **114**, 9538 (1992).
[13] T. Vangberg, R. Lie, and A. Ghosh, J. Am. Chem. Soc. **124**, 8122 (2002).
[14] K. Yoshizawa, T. Nakayama, T. Kamachi, and P. M. Kozlowski, J. Phys. Chem. A **111**, 852 (2007).
[15] H. Hirao, S. Shaik, and P. M. Kozlowski, J. Phys. Chem. A **110**, 6091 (2006).
[16] M. Xiang, G. H. Yao, T. T. Lu, T. J. He, and D. M. Chen, J. Mol. Struct.: THEOCHEM **868**, 6 (2008).
[17] A. M. McKenna, J. M. Purcell, R. P. Rodgers, and A. G. Marshall, Energy Fuels **23**, 2122 (2009).
[18] P. I. Premovic, I. R. Tonsa, M. S. Pavlovic, L. Lopez, and S. LoMonaco, Fuel **77**, 1769 (1998).
[19] M. E. Pena, A. Manjarrez, and A. Campero, Fuel Proc. Tech. **46**, 171 (1996).
[20] C. P. Singh, K. S. Bindra, B. Jain, and S. M. Oak, Opt. Comm. **245**, 407 (2005).
[21] M. Q. Tian, S. Yanagi, K. Sasaki, T. Wada, and H. Sasabe, J. Opt. Soc. Am. B **15**, 846 (1998).
[22] R. A. Timm, M. P. H. Falla, M. F. G. Huila, H. E. M. Peres, F. J. Ramirez-Fernandez, K. Araki, and H. E. Toma, Sensors Actuators B **146**, 61 (2010).
[23] Y. O. Su, R. S. Czernuszewicz, and L. A. Miller, J. Am. Chem. Soc. **110**, 4150 (1988).
[24] K. A. Macor, R. S. Czernuszewicz, and T. G. Spiro, Inorg. Chem. **29**, 1996 (1990).
[25] R. Salcedo, I. P. Zaragoza, J. M. Martinez-Magadan, and I. Garcia-Cruz, J. Mol. Struct.: THEOCHEM **626**, 195 (2003).
[26] S. R. Stoyanov, C. X. Yin, M. R. Gray, J. M. Stryker, S. Gusarov, and A. Kovalenko, J. Phys. Chem. B **114**, 2180 (2010).
[27] Q. Z. Lu, Y. Lu, and J. J. Wang, Chin. J. Chem. Phys. **19**, 227 (2006).
[28] Y. T. Liao, H. Y. Rao, F. F. Kong, and M. B. Luo, Chin. J. Chem. Phys. **18**, 750 (2005).
[29] J. P. Perdew, K. Burke, and M. Ernzerhof, Phys. Rev. Lett. **77**, 3865 (1996).
[30] (a) A. Schaefer, H. Horn, and R. Ahlrichs, J. Chem. Phys. **97**, 2571 (1992).
(b) A. Schaefer, C. Huber, and R. Ahlrichs, J. Chem. Phys. **100**, 5829 (1994).
[31] M. J. Frisch, G. W. Trucks, H. B. Schlegel, G. E. Scuseria, M. A. Robb, J. R. heeseman, G. Scalmani, V. Barone, B. Mennucci, G. A. Petersson, H. Nakatsuji, M. Caricato, X. Li, H. P. Hratchian, A. F. Izmaylov, J. Bloino, G. Zheng, J. L. Sonnenberg, M. Hada, M. Ehara, K. Toyota, R. Fukuda, J. Hasegawa, M. Ishida, T. Nakajima, Y. Honda, O. Kitao, H. Nakai, T. Vreven, J. A. Montgomery, Jr., J. E. Peralta, F. Ogliaro, M. Bearpark, J. J. Heyd, E. Brothers, K. N. Kudin, V. N. Staroverov, T. Keith, R. Kobayashi, J. Normand, K. Raghavachari, A. Rendell, J. C. Burant, S. S. Iyengar, J. Tomasi, M. Cossi, N. Rega, J. M. Millam, M. Klene, J. E. Knox, J. B. Cross, V. Bakken, C. Adamo, J. Jaramillo, R. Gomperts, R. E. Stratmann, O. Yazyev, A. J. Austin, R. Cammi, C. Pomelli, J. W. Ochterski, R. L. Martin, K. Morokuma, V. G. Zakrzewski, G. A. Voth, P. Salvador, J. J. Dannenberg, S. Dapprich, A.

DOI:10.1063/1674-0068/26/05/504-511

D. Daniels, O. Farkas, J. B. Foresman, J. V. Ortiz, J. Cioslowski, and D. J. Fox, *Gaussian 09*, Wallingford CT: Gaussian Inc., (2009).
[32] M. G. B. Drew, P. C. H. Mitchell, and C. E. Scott, Inorg. Chim. Acta **82**, 63 (1984).
[33] S. Hu, C. Y. Lin, M. E. Blackwood, A. Jr. Mukherjee, and T. G. Spiro, J. Phys. Chem. **99**, 9694 (1995).
[34] C. Y. Lin and T. G. Spiro, Inorg. Chem. **35**, 5237 (1996).
[35] K. Czarnecki, L. M. Proniewicz, H. Fujii, D. Ji, R. S. Czernuszewicz, and J. R. Kincaid, Inorg. Chem. **38**, 1543 (1999).
[36] K. Yoshizawa, T. Kato, and T. Yamabe, Chem. Phys. **108**, 7637 (1998).
[37] (a) Y. H. Zhang, W. Zhao, J. Wang, and P. Jiang, Spectrochim. Acta **A75**, 499 (2010).
(b) Y. H. Zhang, W. Zhao, P. Jiang, L. J. Zhang, T. Zhang, and J. Wang, Spectrochim. Acta **A75**, 880 (2010).
[38] T. T. Lu, H. L. Gao, T. J. He, F. C. Liu, and D. M. Chen, Chin. J. Chem. Phys. **23**, 573 (2010).
[39] (a) X. Y. Li, R. S. Czernuszewicz, J. R. Kincaid, Y. O. Su, and T. G. Spiro, J. Phys. Chem. **94**, 31 (1990).
(b) X. Y. Li, R. S. Czernuszewicz, J. R. Kincaid, Y. O. Su, and T. G. Spiro, J. Phys. Chem. **94**, 47 (1990).
[40] T. S. Rush III, P. M. Kozlowski, C. A. Piffat, R. Kumble, M. Z. Zgierski, and T. G. Spiro, J. Phys. Chem. B **104**, 5020 (2000).

DOI:10.1063/1674-0068/26/05/504-511